Spin Exchange of Nitroxyl Radicals in H2O and D2O

ARTICLE *in* THE JOURNAL OF PHYSICAL CHEMISTRY A · DECEMBER 2011

Impact Factor: 2.69 · DOI: 10.1021/jp209755v · Source: PubMed

3 AUTHORS, INCLUDING:

Werner Herrmann
Freie Universität Berlin
26 PUBLICATIONS **362** CITATIONS

SEE PROFILE

THE JOURNAL OF PHYSICAL CHEMISTRY A

ARTICLE

pubs.acs.org/JPCA

Spin Exchange of Nitroxyl Radicals in H_2O and D_2O

Reinhard Stößer,[†] Werner Herrmann,[*,‡] and Anita Pahlke[†]

[†]Institute of Chemistry, Humboldt University Berlin, Brook-Taylor-Strasse 2, D-12489 Berlin, Germany,

[‡]Institute of Pharmacy, Free University Berlin, Kelchstrasse 31, D-12169 Berlin, Germany

ABSTRACT: By means of continuous wave electron spin resonance (cw ESR) in the X and L bands, the spin exchange of series of different concentrations of the spin probes 2,2,6,6-tetramethylpiperidine-1-oxyl (TEMPO), 4-hydroxy-2,2,6,6-tetramethylpiperidine-1-oxyl (TEMPOL), and 4-(trimethylamino)-2,2,6,6-tetramethylpiperidine-1-oxyl iodide (CAT-1) in H_2O and D_2O have been examined. The rate constants k_e of the spin exchange have been determined by complete spectra simulations, as well as directly from hyperfine line broadenings and concentration depending line shifts. The obtained results showed a good agreement. Their respective differences $\{k_e(H_2O) - k_e(D_2O)\}$ could be determined for the first time. They reflect the different influence of the solvents on the spin dynamics but confirm the decrease of the reaction rate in D_2O, caused by the higher degree of order in this liquid. The spectroscopic and kinetic results presented in this paper establish a further kind of isotopic effect.

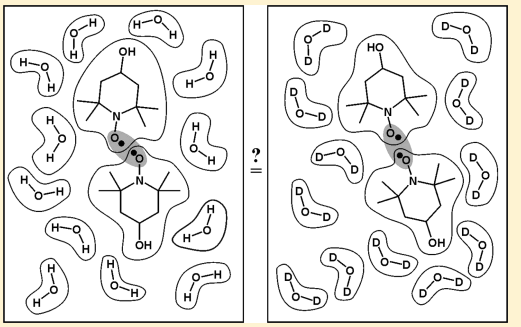

INTRODUCTION

Water is one of the most important substances of all. Not only does it serve as a "working fluid" in machines and devices for transforming energy, it is the most frequently used solvent and it plays an important role in weather and climate phenomena and, finally, in all processes inside of living organisms.

The properties of the system H_2O/D_2O are probably the best examined ones compared to other fluid pairs of isotopes.

In nature, as well as in the laboratory and in industry, many chemical reactions proceed in water. The specific properties of these systems reveal among others in about 40 anomalies.[1,2] Additionally, interesting isotopic effects occur; e.g., H_2O and D_2O (T_2O is not mentioned) differ in some physical and chemical properties, in particular in the temperature range $-30\ ^\circ C < T < 30\ ^\circ C$.

Despite the large number of experimental and theoretical examinations of the physicochemical properties of water, the recent knowledge about anomalies[1−3] including the isotopic effects is still insufficient.

By means of thermodynamic, in particular differential scanning calorimetry (DSC), diffraction investigations,[4] and finally vibrational and nuclear magnetic resonance (NMR) spectroscopic methods allowed the development of fundamental insights into the phase behavior and, thus, the changes in properties.

One of the very interesting properties of water is the formation of clathrates with organic molecules using a special (T, p) regime.[5−7] There is a certain connection to the subject of the present work because it also touches the incorporation of organic spin probes into H_2O and D_2O, respectively. Some parallels can be established between the influence of the organic spin probes and organic molecules (e.g., of *tert*-butyl methyl ether) on the structure of the surrounding water.

With respect to the topic of the present paper, there are chemical and biological findings,[8] which have smaller reaction rates in D_2O than in H_2O.[1,2]

At first, it seems to be strange to use ESR spectroscopy for examining properties of water, and the characterization of differences between H_2O and D_2O, respectively. The comparatively high sensitivity and selectivity of the ESR method[9,10] could be used to advance into the "no man's land" of the phase diagram of water,[11] where other methods obviously failed. Moreover, ESR spectroscopy succeeded in getting new insights in the glass transition and structure relaxation of water,[12] as well as in the process of freezing.[13,14]

Isotopic effects, in particular the exchange of ^1H by ^2H, have been used in ESR for a long time already. For example, there are clear differences in the hyperfine couplings of $-\underset{|}{\overset{}{R}}-{}^1H-$ or $-\underset{|}{\overset{\cdot}{R}}-{}^2H-$, respectively, due to the different nuclear moments of ^1H and ^2H. Such substitutions are successfully applied on investigating the origin of ^1H in radicals, or more general on signal assigning.

A new isotopic effect concerning the different recombination efficiencies for radical pairs containing different isotopes of a certain element, the magnetic isotope effect, was discovered by Molin and Salikhov et al.[15]

Up to now, the potentially different influence of the molecules H_2O and D_2O on the parameters of ESR spectra has been used for determining coordinative effects in metal complexes, or on examining the lifetime of excited triplet states.

Generally, isotopic effects can be observed if a reaction rate or an equilibrium constant changes as a result of a change of

Received: October 11, 2011
Revised: December 5, 2011
Published: December 16, 2011

isotopes. Therefore, such a substitution can be used to gain insight in structures and reactivity.[8] Thus, the mass and nuclear spin depending properties of the H_2O/D_2O system are reflected in their vibrational and NMR spectra. In ESR spectroscopy the spin exchange of paramagnetic species can be used as a comparatively simple but very informative approach to "reaction rates".[9,16]

Being a preliminary stage of a chemical reaction, the spin exchange delivers information about the different interactions of the spin probe molecules with those of the solvent by means of the values of the rate constant k_e. The reason for that can be seen within the phenomenon of spin exchange itself. Collisions of spin probe molecules surrounded by the solvent molecules can lead to an exchange of valence electrons on keeping the electron spin, thus exchanging the spins between the respective atoms. That fundamental collision activity takes place in every chemical reaction of paramagnetic molecules in a large number and is determined by the viscosity, the temperature, and the concentration of the particles. The kinetic interpretation[16] of these collisions leads to k_e values, which are average values of the sample but they are sensitive enough to reflect the influence of the solvent.

The examination of the spin exchange of paramagnetic molecules in solution[9,16−21] by means of ESR allows specific views on the dynamics of the systems, and in particular on the first stages of the interactions between radicals, which finally can lead to bimolecular reactions; i.e., we can find a relation to the contribution of nonreactive collisions, or the temporary formation of aggregates or cages in solution, respectively.

Today one can find a larger number of papers concerning the spin exchange in solutions using models of different origin for the interpretation of the experimental results.[9,16−19,22]

Within the context of the dynamics of stable nitroxyl radicals in conventional solvents,[23] ionic liquids,[24] and biological objects, several models for interpreting the experimental findings have been used to discuss their applicability.[9] It could be shown that parameters of spin exchange such as k_e and the activation energy of the spin exchange ΔE_a agree in an acceptable manner, whether they are obtained by complete spectrum simulation,[25] or by relations between k_e and line broadening and line shifts.[19] Spectrum simulations have the advantage that they provide rotational correlation times additionally.

Although the influence of solvents, including H_2O, on the parameters of ESR spectra is discussed in many papers, the comparison H_2O/D_2O seems to be nearly unknown.

Thus the present paper will provide the results of the examinations of varying concentrations of three spin probes in H_2O and D_2O by means of cw ESR in the X and L band at 293 K.

The investigations should answer the question, if the tools used (i.e., the experimental techniques combined with the models for simulation and evaluation) are able to differentiate in between the interactions of the spin probes with H_2O or D_2O, respectively. Furthermore, it was of interest to give evidence for the differences in behavior of the spin probes with their substituents (−H, −OH, and $-NR_3^+$) in position 4 (Figure 1) concerning the static (A_{iso}) and dynamic parameters in aqueous solutions. The L band examinations shall serve to ensure the X band results or to find further differences, respectively.

As the results show, the asked questions could be answered by means of quantifying the spin exchange.

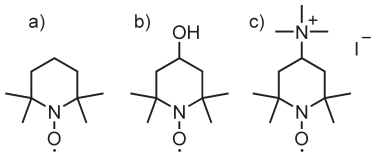

Figure 1. Spin probes (a) 2,2,6,6-tetramethylpiperidine-1-oxyl (TEMPO or TMP, respectively), (b) 4-hydroxy-2,2,6,6-tetramethylpiperidine-1-oxyl (TEMPOL or TOL, respectively), and (c) (trimethylamino)-2,2,6,6-tetramethylpiperidine-1-oxyl iodide (CAT-1 or CAT, respectively).

MATERIALS AND METHODS

The spin probes TEMPO and TEMPOL were bought from Sigma-Aldrich, whereas CAT-1 was purchased from the Institute of Organic Chemistry of the Russian Academy of Sciences, Novosibirsk.

The ESR spectroscopic investigations in X band have been done using a spectrometer ERS 300 (ZWG Adlershof, Magnettech Ltd., Berlin, Germany) whereas for the L band the aforementioned spectrometer has been equipped with a microwave bridge MWU-L6 (Magnettech Ltd., Berlin, Germany). The microwave frequencies were 9.25 and 1.43 GHz, respectively.

The collected data of Table 1 as representation of different solvent properties should be of potential influence on the ESR spectra of the dissolved spin probes.

As it will be shown, there is a rather measurable influence on the dynamic parameters τ_R (reorientation correlation time) and k_e (rate constant of the spin exchange) than on static spin Hamiltonian parameters such as $\hat{g}$ and $\hat{A}$.

The ESR spectra were analyzed in three ways:

(i) Determination of the exact line positions and extrema of the intensity, i.e., the determination of hyperfine coupling constants and line widths for all concentrations of the used spin probes (Table 2).

(ii) Calculation of the spin exchange rate constants k_e, based on the formulas[9,19]

$$k_e = 1.52 \times 10^7 \frac{g}{2(1-\varphi)} \frac{\Delta B}{C} \quad (1)$$

$$k_e = 1.76 \times 10^7 \frac{g}{2\sqrt{\varphi}} \frac{\sqrt{A_{iso} \cdot \delta A_{iso}}}{C} \quad (2)$$

k_e = spin exchange rate constant in $L \cdot mol^{-1} \cdot s^{-1}$
g = g factor
ΔB = exchange line broadening
φ = statistical weight of the ESR line (2/3 for ^{14}N)
C = concentration $mol \cdot L^{-1}$
A_{iso} = hyperfine splitting with $\delta A_{iso} = A_{iso}^0 - A_{iso}$ and A_{iso}^0 being the hyperfine splitting without spin exchange
Equation 1 makes use of the line broadening effects, and eq 2 takes line shifts into account.

(iii) Simulations of the complete spectra on the basis of ref 25 provide values for the reorientation time τ_R, the exchange parameter ω_{ss}, and derived from them values for the rate constant k_e (Table 3).

RESULTS

The ESR spectra of the solutions containing different concentrations of the spin probes in H_2O and D_2O have been

Table 1. Selected Properties of H_2O and D_2O[1,31,32]

		H_2O	D_2O	X_{D_2O}/X_{H_2O}
density at 25 °C	$g \cdot cm^{-3}$	0.99701	1.1044	1.108
viscosity at 25 °C	mPa·s	0.895	1.113	1.244
electric dipole moment at 20 °C	Debye	1.76	1.78	1.011
ionic conductivity of X_3O^+	$cm^2 \cdot \Omega^{-1} \cdot mol^{-1}$	349.8	250.1	0.715
solubility of NaCl at 25 °C	$g \cdot L^{-1}$	359	300	0.836
electric conductivity	$\mu S \cdot cm^{-1}$	0.0635		
dielectric constant at 25 °C		78.304	77.937	0.995
C_p	$cal \cdot deg^{-1} \cdot mol^{-1}$	17.99	20.16	1.121
C_v	$cal \cdot deg^{-1} \cdot mol^{-1}$	17.80	20.0	1.124
refractive index	n_D^{20}	1.3326	1.3283	0.997
surface tension	$N \cdot m^{-1}$	0.07197	0.07193	0.999

recorded in the X and L bands at 293 K, and a selection is displayed in Figure 4.

Without further means, the influence of the respective spin probe concentration can be recognized easily by inspection of the amplitudes and line widths of the individual hyperfine lines. With increasing spin probe concentrations the values of the molecular reorientation τ_R increase (Table 3), as well as the line widths of the individual hyperfine lines, and a decrease of the ^{14}N hyperfine coupling constants can be observed (Table 2). Moreover, Figure 4 depicts the line shifts of the hyperfine lines as a clear manifestation of the decreasing hyperfine splitting. The latter effects are caused by the spin exchange of the spin probe molecules.

The ΔB (line broadening) and A_{iso} (hyperfine splitting) values determined directly from the ESR spectra are summarized in Table 2. It is interesting to note that the A_{iso} values of the system TEMPO/D_2O are larger than those of TEMPO/H_2O. The differences increase with the concentration of the spin probe due to the increasing efficiency of the spin exchange and, thus, the averaging of the hyperfine structure progresses. That process is less efficient in D_2O.

According to a rather phenomenological aspect some tendencies with respect to line broadening and splitting can be observed, which are summarized in Tables 4 and 5 and Figures 2 and 3. Observing the changes of the line widths $\delta\Delta B$ of the individual hyperfine lines and the hyperfine coupling constants δa (Figure 2) with dependency on the concentration of the spin probes, the respective fluid matrix (H_2O or D_2O), and the microwave frequency (X or L band), one can see these interconnections (Figures 2 and 3).

It can be stated that TEMPO shows a relatively strong dependency on the kind of solvent and microwave frequency, whereas the dependency of the more polar spin probes TEMPOL and CAT-1 is smaller. This is also true for the effects of line shift and the concentration depending hyperfine splitting δa. As expected on the basis of the phenomenon of spin exchange, there is a mutual dependency between the parameters $\delta\Delta B$ and δa.

The complete spectral simulation by means of the algorithm according to Budil et al.[25] supplies the values for τ_R and k_e as displayed in Table 3. It should be mentioned here that fitting the calculated to the recorded spectra delivers very good agreements (due to the good agreements the simulated spectra are omitted in Figure 4).

The quality of the simulation can be seen not only in the good agreement between the experimental and the simulated spectra but also in the values of spin-Hamiltonian parameters $\hat{g}$ (as the components g_x, g_y, and g_z) and $\hat{A}$ (as the components A_x, A_y, and A_z), which have been used for the simulation, that fit perfectly to the corresponding isotropic values of the experimental spectra.

As mentioned above, the experimental spectra have been examined concerning the concentration induced changes of line widths and line shifts. The results are displayed in Table 3 and the obtained values for the spin exchange k_e correspond with those from the complete spectra simulations. A similar connection has been described for other liquid systems such as *n*-octanol and the ionic liquid 1-methyl-3-octylimidazolium hexafluorophosphate in ref 9.

That means, because of the good agreement between the results of the simulation and the analysis of the parameters of the experimental spectra, we conclude that the effects of line broadening and line shift are mainly determined by the spin exchange.

The complete spectra simulation of the experimental spectra supplies values for the parameters τ_R and ω_{ss} (including the derived values for k_e), and these are summarized in Table 3, including the k_e values obtained using the formulas 1 and 2[9,18] and, moreover, the re-encounter times τ_{RE}.[26]

With respect to the goal of the paper, the differences in the rate constants of the spin exchange for the three spin probes in H_2O and D_2O are given in Table 6 (the given mean values are for orientation purposes only; the values are obtained using different models, thus giving large σ values), clearly showing the isotope effect on the spin exchange.

DISCUSSION

In the following some aspects of the connection between spectral patterns and microscopic properties of the solvents will be discussed.

As Figure 4 shows, the ESR spectra of the spin probes differ only slightly for the concentration of 1 mM. At concentrations of about 25 mM there are clear line broadenings and line shifts. For TEMPO, which is already near the limit of solubility at that concentration, the strongest effects are observed. Moreover, increasing the concentrations of CAT-1 and TEMPOL to about 100 mM leads to stronger $\delta\Delta B$ and δa effects, as can be seen in Figure 4. Still higher concentrations (250 mM) could be achieved for TEMPOL only. TEMPOL in both solvents at that concentration leads to ESR spectra that are characterized by the complete collapse of the hyperfine triplet and only a single line can be observed. It means the spin exchange is very effective under these conditions.

Summarizing the findings as displayed in Figure 4 and those values for k_e obtained by the calculations according to the

dx.doi.org/10.1021/jp209755v | J. Phys. Chem. A 2012, 116, 952–961

Table 2. Line Widths ΔB (G) and Isotropic Hyperfine Coupling A_{iso} (G) Constants, Determined from the Experimental ESR Spectra (293 K), Recorded in X- and L-Band for the Spin Probes TEMPO, TEMPOL, and CAT-1 in H_2O and D_2O

TEMPO in H_2O, X-Band			TEMPO in D_2O, X-Band		
conc (mM)	ΔB (G)	A_{iso} (G)	conc (mM)	ΔB (G)	A_{iso} (G)
			34	3.65	16.36
22	3.46	16.43	25	2.84	16.67
10	2.00	16.95	10	1.66	17.06
5	1.50	17.11	5	1.39	17.16
2.5	2.66	17.19	2.5	1.31	17.19
1	1.37	17.23	1	1.28	17.21
0.5	1.27	17.20	0.5	1.28	17.20
TEMPO in H_2O, L-Band			TEMPO in D_2O, L-Band		
conc (mM)	ΔB (G)	A_{iso} (G)	conc (mM)	ΔB (G)	A_{iso} (G)
			34	3.21	16.59
22	3.64	16.42	25	2.48	16.79
10	1.77	16.98	10	1.50	17.08
5	1.37	17.13	5	1.37	17.12
2.5	1.34	17.12	2.5	1.31	17.17
1	1.33	17.19	1	1.33	17.19
0.5	1.28	17.19	0.5	1.23	17.18
TEMPOL in H_2O, X-Band			TEMPOL in D_2O, X-Band		
conc (mM)	ΔB (G)	A_{iso} (G)	conc (mM)	ΔB (G)	A_{iso} (G)
100	6.5	14.39	100	6.83	13.95
75	4.89	15.60	75	5.98	14.84
50	2.93	16.48	50	4.49	15.83
25	1.93	16.84	25	2.76	16.53
10	1.71	16.88	10	1.89	16.84
5	1.66	16.94	5	1.71	16.90
2.5	1.64	16.95	2.5	1.65	16.95
			1	1.64	16.96
			0.5	1.60	16.95
TEMPOL in H_2O, L-Band			TEMPOL in D_2O, L-Band		
conc (mM)	ΔB (G)	A_{iso} (G)	conc (mM)	ΔB (G)	A_{iso} (G)
			100	7.19	14.11
75	7.03	14.55	75	6.07	15.00
50	4.09	15.95	50	4.69	15.74
25	3.01	16.55	25	2.90	16.56
10	1.88	16.85	10	1.96	16.81
5	1.81	16.87	5	1.74	16.90
2.5	1.60	16.94	2.5	1.66	16.95
1	1.61	17.03	1	1.65	16.93
0.5	1.71	16.83	0.5	1.74	16.97
CAT-1 in H_2O, X-Band			CAT-1 in D_2O, X-Band		
conc (mM)	ΔB (G)	A_{iso} (G)	conc (mM)	ΔB (G)	A_{iso} (G)
88.7	6.72	14.05	94	6.17	14.57
75	6.13	14.68	75	5.24	15.30
50	4.45	15.67	50	3.81	15.99
25	2.62	16.40	25	2.36	16.48
10	1.81	16.64	10	1.77	16.65
5	1.66	16.68	5	1.65	16.69
2.5	1.65	16.71	2.5	1.66	16.71
1	1.63	16.74	1	1.63	16.72
0.5	1.65	16.74	0.5	1.65	16.74
CAT-1 in H_2O, L-Band			CAT-1 in D_2O, L-Band		
conc (mM)	ΔB (G)	A_{iso} (G)	conc (mM)	ΔB (G)	A_{iso} (G)
88.7	6.75	14.34	94	6.72	14.45
75	3.51	15.93	75	5.10	15.45
50	4.40	15.81	50	3.61	16.09
25	2.63	16.40	25	2.33	16.51
10	1.75	16.69	10	2.33	16.51
5	1.69	16.63	5	1.71	16.69
2.5	1.67	16.68	2.5	1.67	16.72
1	1.67	16.72	1	1.72	16.69
0.5	1.61	16.70	0.5	1.69	16.68

formulas 1 and 2 and spectra simulations using the Budil algorithm[25] gives a somewhat unexpected result. Although the limit of solubility of TEMPO in both solvents is reached, no collapse of the hyperfine lines is observed. This is in formal contrast to the findings for TEMPOL (Figure 4). The elucidation of this effect can be given in the following way. On decreasing solubility of the spin probes (TEMPO and partly CAT-1) the increasing tendency to form aggregates of the spin probes should lead to the collapse of the hyperfine lines. But the thermal fluctuations of the solvent structures under discussion[3,27,28] prevent the formation of rather stationary hydrophobic bonds. The highest probability should be with TEMPO. That nonpolar spin probe with its limited solubility in polar solvents is able to undergo van der Waals interactions with H_2O, or D_2O, respectively, but partly forms hydrogen bonds with the >NO$^{\bullet}$ group, as well as dipole interactions and, thus, can reach higher k_e values, too. But its disposition to aggregation is not very strong, despite its k_e values being the largest of the three spin probes (Table 3).

At this point one has to keep in mind that the spin exchange constant k_e (in $L \cdot mol^{-1} \cdot s^{-1}$) represents a kinetic process of second order. Therefore, the spectral effect strongly depends on the actual concentration of the colliding radicals. In principal, such a tendency can be considered to be the borderline to dimer formation, or due to the low polarity of the spin probe as a precursor of a hydrophobic bond.[28] For the last case the TEMPO molecule seems to be too small, because the formation of such a bond would lead to the reduction of the translational and rotational contributions to the entropy, and thus, the driving force to bond formation would be too small.[28] Nevertheless, even in that case of smaller solubility of TEMPO one should expect a larger probability of encounters of the molecules, causing a higher spin exchange (see also the re-encounter times τ_{RE}).

It can be assumed that the water molecules solvatize the dissolved "guest" molecules on forming cages around these

dx.doi.org/10.1021/jp209755v |J. Phys. Chem. A 2012, 116, 952–961

Table 3. Survey of the τ_R and ω_{ss} Values, Obtained by Applying the Algorithm According to Budil et al.[25] and the Derived Values for k_e, Compared to Those, from the Experimental ESR Spectra (293 K), Recorded in X- and L-Band for the Spin Probes TEMPO, TEMPOL, and CAT-1 in H_2O and D_2O

TEMPO in H_2O					TEMPO in D_2O				
conc (mM)	τ_R (ns)	ω_{ss} (10^{-9} s^{-1})	k_e[a]	k_e[b]	conc (mM)	τ_R (ns)	ω_{ss} (10^{-9} s^{-1})	k_e[a]	k_e[b]
					34	22.91	0.060	1.77×10^9	2.43×10^9
22	8.87	0.039	1.79×10^9	4.67×10^9	25	14.29	0.044	1.77×10^9	2.75×10^9
10	0.56	0.036	3.64×10^9	4.22×10^9	10	2.03	0.003	3.35×10^8	5.27×10^9
5	0.11	0.016	3.27×10^9	5.65×10^9	5	0.39	0.00001		6.92×10^9
2.5	0.12	0.00065	2.61×10^8	8.76×10^9	2.5	0.24			9.86×10^9
1	0.10	0.00027			1	0.21			1.60×10^{10}
0.5	0.16	0.00038			0.5	0.2			--

TEMPO in H_2O				TEMPO in D_2O			
conc (mM)	τ_{RE} (ns)	k_e[c]	k_e[d]	conc (mM)	τ_{RE} (ns)	k_e[c]	k_e[d]
				34	2.471	1.60×10^9	3.36×10^9
22	2.411	2.27×10^9	4.94×10^9	25	2.517	1.43×10^9	3.67×10^9
10	2.726	1.67×10^9	6.34×10^9	10	3.429	8.92×10^8	4.88×10^9
5	3.56	1.06×10^9	7.56×10^9	5	4.864	5.57×10^8	5.92×10^9
2.5	0.003		6.22×10^9	2.5	11.19	3.35×10^8	8.05×10^9
1	2.305	2.23×10^9		1			
0.5				0.5			

TEMPOL in H_2O					TEMPOL in D_2O				
conc (mM)	τ_R (ns)	ω_{ss} (10^{-9} s^{-1})	k_e[a]	k_e[b]	conc (mM)	τ_R (ns)	ω_{ss} (10^{-9} s^{-1})	k_e[a]	k_e[b]
150	32.81	0.156	1.04×10^9	1.59×10^9	150	18.88	0.151	1.01×10^9	1.47×10^9
138	43.65	0.195	1.42×10^9	1.39×10^9	138	29.65	0.147	1.06×10^9	1.51×10^9
100	4.33	0.180	1.80×10^9	1.23×10^9	100	33.57	0.124	1.24×10^9	1.68×10^9
75	7.05	0.121	1.61×10^9	1.96×10^9	75	7.14	0.121	1.62×10^9	1.38×10^9
50	1.03	0.110	2.20×10^9	1.40×10^9	50	2.07	0.084	1.69×10^9	1.67×10^9
25	1.04	0.047	1.87×10^9	2.59×10^9	25	1.43	0.051	2.06×10^9	2.10×10^9
10	0.45	0.026	2.55×10^9	3.05×10^9	10	2.41	0.021	2.13×10^9	3.57×10^9
5	0.76	0.010	1.93×10^9	6.10×10^9	5	2.13	0.008	1.77×10^9	6.10×10^9
2.5	0.73	0.006	2.37×10^9	8.85×10^9	2.5	0.6	0.007	2.78×10^9	5.51×10^9
1	0.96	0.002	1.71×10^9	1.78×10^{10}	1	0.52	0.006	6.18×10^9	7.95×10^9

TEMPOL in H_2O				TEMPOL in D_2O			
conc (mM)	τ_{RE} (ns)	k_e[c]	k_e[d]	conc (mM)	τ_{RE} (ns)	k_e[c]	k_e[d]
100	4.895	1.11×10^9	1.85×10^9	100	5.873	1.19×10^9	1.98×10^9
75	3.228	9.88×10^8	1.87×10^9	75	4.152	1.33×10^9	2.28×10^9
50	2.916	5.91×10^8	1.71×10^9	50	2.928	1.32×10^9	2.59×10^9
25	3.372	2.67×10^8	1.66×10^9	25	3.083	1.06×10^9	3.27×10^9
10	25.538	1.67×10^8	3.42×10^9	10	4.714	6.69×10^8	4.51×10^9
5	9.266	1.11×10^8	3.05×10^9	5	11.311	5.02×10^8	6.89×10^9
2.5				2.5	1.018	4.46×10^8	5.00×10^9
1				1			
0.5				0.5			

CAT-1 in H_2O					CAT-1 in D_2O				
conc (mM)	τ_R (ns)	ω_{ss} (10^{-9} s^{-1})	k_e[a]	k_e[b]	conc.(mM)	τ_R (ns)	ω_{ss} (10^{-9} s^{-1})	k_e[a]	k_e[b]
88.7	42.36	0.135	1.52×10^9	1.40×10^9	94	68.08	0.133	1.42×10^9	9.12×10^8
75	31.48	0.091	1.22×10^9	2.00×10^9	75	51.29	0.096	1.28×10^9	1.16×10^9
50	7.89	0.080	1.60×10^9	1.51×10^9	50	76.56	0.062	1.23×10^9	1.38×10^9

dx.doi.org/10.1021/jp209755v |J. Phys. Chem. A 2012, 116, 952–961

Table 3. Continued

CAT-1 in H_2O					CAT-1 in D_2O				
conc (mM)	τ_R (ns)	ω_{ss} (10^{-9} s^{-1})	k_e[a]	k_e[b]	conc.(mM)	τ_R (ns)	ω_{ss} (10^{-9} s^{-1})	k_e[a]	k_e[b]
25	9.89	0.037	1.49×10^9	1.94×10^9	25	21.23	0.025	9.84×10^8	2.13×10^9
10	3.98	0.013	1.26×10^9	2.92×10^9	10	2.88	0.009	9.12×10^8	2.92×10^9
5	2.94	0.00002		4.46×10^9	5	16.52			5.34×10^9
2.5	2.52	0.000007		5.69×10^9	2.5	4.73			8.49×10^9
1	2.09			1.58×10^{10}	1	0.84			
0.5	0.88				0.5	0.49			

CAT-1 in H_2O				CAT-1 in D_2O			
conc (mM)	τ_{RE} (ns)	k_e[c]	k_e[d]	conc (mM)	τ_{RE} (ns)	k_e[c]	k_e[d]
88.7	4.891	1.23×10^9	1.99×10^9	94	3.856	1.11×10^9	1.81×10^9
75	3.640	1.36×10^9	2.23×10^9	75	2.705	1.10×10^9	1.90×10^9
50	2.768	1.28×10^9	2.49×10^9	50	2.133	1.00×10^9	2.07×10^9
25	2.801	8.80×10^8	2.88×10^9	25	2.281	6.80×10^8	2.40×10^9
10	9.755	3.62×10^8	3.93×10^9	10	4.095	3.62×10^8	3.17×10^9
5	504.248	5.56×10^7	5.86×10^9	5	11.521	1.67×10^8	3.97×10^9
2.5			8.66×10^9	2.5	0.258	4.46×10^8	3.54×10^9
1				1			
0.5				0.5			

[a] Based on the results for the spin exchange according to calculations using the Budil algorithm. [b] Based on the changes in the hyperfine splitting according to calculations using the Budil algorithm. [c] Based on the changes in the hyperfine splitting as determined from the experimental spectra. [d] Based on the line broadening due to spin exchange as determined from the experimental spectra.

Table 4. Line Widths $f(C)$ δ Slope (%)

	H_2O-X	H_2O-L	D_2O-X	D_2O-L
TEMPOL	51	51	45.9	46.1
TEMPO	100	(109.8)	71.8	62.2
CAT-1	46.9	38.7	38.7	39.0

Table 5. Hyperfine Coupling Constants $f(C)$ δ slope (%)

	H_2O-X	H_2O-L	D_2O-X	D_2O-L
TEMPOL	100	83	83.3	74.8
TEMPO	76.1	87.8	55.9	45.6
CAT-1	79.9	58.8	54.1	54.9

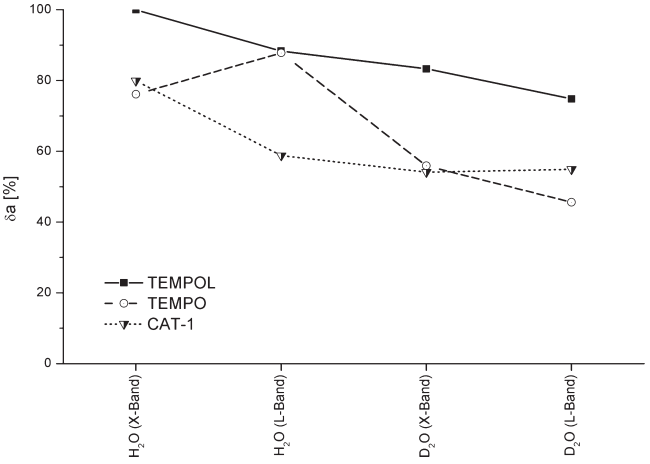

Figure 2. Dependency of the relative line shift δa of the three hyperfine lines of the spin probes as a function of the microwave frequency and the solvent used.

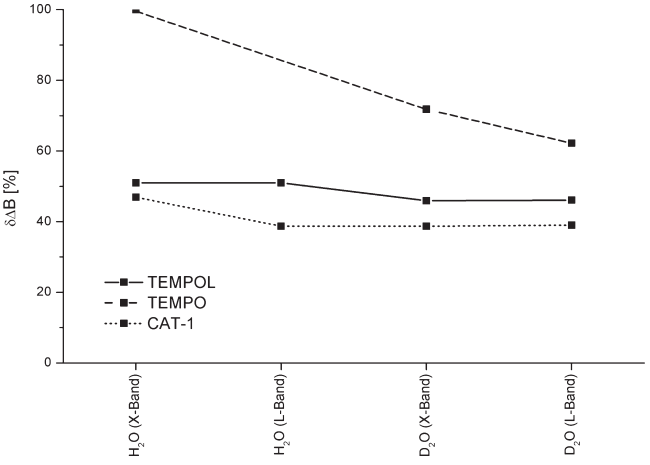

Figure 3. Dependency of the relative line broadening $\delta\Delta B$ of the three hyperfine lines of the spin probes as a function of the microwave frequency and the solvent used.

partially hydrophobic spin probe molecules. On that, the shape of the cages generally follows the geometry of the solute.

In particular, attracting interactions between solute and water molecules are formed if there are atoms with free pairs of electrons in the "guest" molecules. Such interactions disturb the structure of the cage around the solute and result in a partially higher solubility and diffusivity of the solute in H_2O and D_2O, respectively, as could be observed for the spin probe TEMPOL. Vice versa, the hydrophobic contribution to the interactions between a more hydrophobic solute (e.g., TEMPO) limits the guest−host contact and a more strongly hydrogen-bonded network of water molecules around the solute results. In other

dx.doi.org/10.1021/jp209755v |J. Phys. Chem. A 2012, 116, 952–961

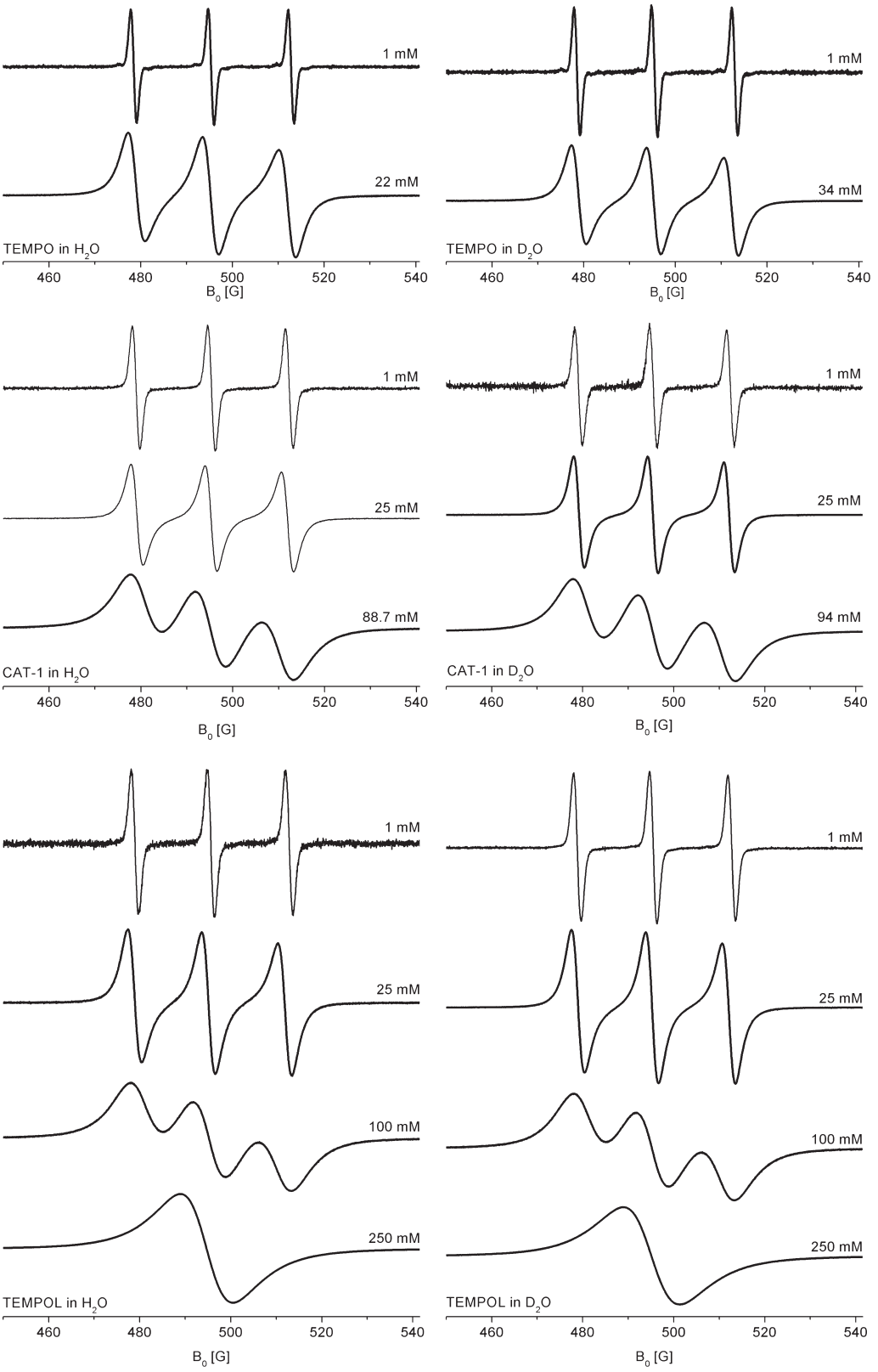

Figure 4. ESR L-Band spectra of the spin probes CAT-1, TEMPOL, and TEMPO dissolved in H_2O (left) and D_2O (right) recorded at 293 K. The concentrations of the spin probes range from 1 to 250 mM.

words, the water will be more structured. The border case could be the formation of "iceberg structures".

The lower polarity of the TEMPO molecule partly forces the H_2O and D_2O to form "iceberg structures"[3,27,28] or precursors

Table 6. Rate Constants $10^{-9}k_e$ ($L \cdot mol^{-1} \cdot s^{-1}$) for the Spin Probes TEMPO, TEMPOL, and CAT-1 in H_2O and D_2O

	H_2O X-Band	H_2O L-Band	D_2O X-Band	D_2O L-Band	Δ X-Band(H_2O-D_2O)	Δ L-Band(H_2O-D_2O)
TEMPO	4.2226[a]		1.86252		2.3601	
	1.14947[b]		2.40814		−1.2587	
	2.36542[c]	3.14095	1.78868	1.39429	0.5767	1.7467
	4.55342[d]	3.88975	2.96925	2.33825	1.5842	1.5515
	3.29; σ 1.6		2.14; σ 0.55		1.57; σ 0.53	
TEMPOL	1.25608[a)]		1.35259		−0.0965	
	1.48704[b]		0.9962		0.4908	
	1.94346[c]	1.7246	1.29291	1.347	0.6506	0.3776
	1.42843[d]	1.95324	(−2.5432 × 10^7)	1.66749		0.2858
	1.46; σ 0.29		1.29; σ 0.19		0.38; σ 0.28	
CAT-1	1.6899[a]		0.905386	0.7696	0.7845	
	1.41609[b]		1.4652	0.0491	−0.0491	
	1.44579[c]	1.4613	1.19416	1.42991	0.2516	0.0314
	1.93153[d]	1.9281	(−2.1112 × 10^7)	1.71565		0.2125
	1.57; σ 0.24		1.19; σ 0.28		0.21; σ 0.32	

[a] k_e determined from the concentration-depending line broadening calculated using the Budil algorithm.[25] [b] k_e determined from the concentration-depending exchange parameter calculated using the Budil algorithm.[25] [c] k_e determined from the concentration-depending line broadening using formula 1. [d] k_e determined from the concentration-depending line shift calculated using formula 2.

of them, which are thermodynamically favored because of their enlarged numbers of hydrogen bonds. That leads in the case of the dissolved spin probe to a reduction in the number of interchanging water molecules interacting with the spin probe and probably results in a locally higher spin probe concentration (thus, shorter distances between the spin probe molecules), which favors the spin exchange. If the number of interacting water molecules decreases, the "micropolarity" decreases, too, and thus the value of the hyperfine coupling constant A_{iso}.[29] Moreover, the spin exchange will change in the same direction. Another aspect in favor of spin exchange can be seen in the fact that the structures of the solvent fluctuate because of the available thermal energy with time constants of 10^{-10} to 10^{-11} s (compare the k_e values of Table 3).[27]

Due to the selected experimental conditions a further increase of the concentration of TEMPO in H_2O and D_2O is not possible without external forces; thus k_e could only be increased by raising the temperature,[9] and therefore we can just observe a distinctive line broadening and line shifts, without the total collapse of the hyperfine triplet at 293 K. The necessary concentration for that collapse can also not be achieved locally, and even the higher spin exchange rate compared to those of CAT-1 and TEMPOL (Table 5) is not sufficient to average out the hyperfine structure at a concentration of about 30 mM.

That will be different with the spin probe TEMPOL. Due to the −OH substituent in position 4 of the piperidine structure (Figure 1) the spin probe molecules will be embedded into the fluctuating network of hydrogen bonds in the solvents H_2O and D_2O, respectively. These directed interactions (hydrogen bridges)[30] of the spin probe are supported by additional interactions as mentioned for the spin probe TEMPO. This will increase the solubility remarkably. The average distances between the spin probe molecules rather correspond to the (macroscopic) concentration of the probe, and spin exchange takes place efficiently, whereas its value is smaller than that of TEMPO. The resulting higher degree of order of the solution diminishes the effect of spin exchange of TEMPOL. But due to the possibility to increase the spin probe concentration considerably, it finally leads to the collapse of the hyperfine triplet (Figure 4).

The behavior of the spin probe CAT-1 in an aqueous system will be influenced by its charge. The solubility is increased because of additional enthalpy effects, caused by interactions between the ions of the spin probe and water dipoles. However, the efficiency of the spin exchange will be partly reduced due to Coulomb repulsion forces between the radical ions. On the other hand, the ions break the structure of the aqueous system. The value of the spin exchange constant k_e reflects the totality of all these effects (Table 3). With its solubility between TEMPO and TEMPOL, one can observe a considerable line broadening and line shifts, but the spin exchange is not sufficient to average out the hyperfine splitting completely (Figure 4).

Besides these rather semiquantitative conclusions, the k_e values provide quantitative statements concerning the interaction of the spin probes in H_2O and D_2O (Table 3). The different properties of H_2O and D_2O can be clearly seen in the differences $\{k_e(H_2O) - k_e(D_2O)\}$ (Table 6), mainly caused by the differences in viscosity and density of both solvents together with the more structured state of the liquid D_2O.

Contrary to that, the values for the differences in the isotropic hyperfine couplings A_{iso}, which can only be evaluated for low concentrations in H_2O and D_2O, respectively, are extremely small. Obviously, the applied experimental method does not provide the adequate spectral resolution.

As it is known, the macroscopic yields of chemical reactions in D_2O are smaller than those in H_2O.[8,31−33] This is true for the spin exchange, too, despite the differences of the static spin-Hamiltonians (e.g., $\hat{g}$ and $\hat{A}$) are very small and no chemical product is formed. Thus, the presented spectroscopic results are an evidence for further up to now unknown isotopic effects.

CONCLUSIONS

Several differences in physical and chemical properties of H_2O and D_2O have been found experimentally up to now. They have been shown to be relatively small. Even the respective phase diagrams do not show large differences.[11]

In other words, the physical properties of H_2O and D_2O are very similar and it requires very accurate and elaborate

dx.doi.org/10.1021/jp209755v | J. Phys. Chem. A 2012, 116, 952–961

examinations to quantify the differences. If one considers that viscosity (26% difference) and density (11% difference) are rather different (Table 1), then it may be assumed that D_2O will be the more structured liquid. The reason can be seen in the stronger hydrogen bonds in D_2O. Moreover, measurements of properties of micelles in both systems have shown that the average degree of aggregation is larger in D_2O.[3,34]

Contrary to the great number of examinations under equilibrium conditions, kinetic studies offer the opportunity to differentiate between the different interactions of dissolved molecules, or aggregates, respectively, in H_2O and D_2O. Thus, by means of NMR relaxation it was found that the formation of micelles, and disintegration, respectively, proceed 3 times slower in D_2O than in H_2O.[3,34]

Considering spectroscopic aspects, the differences in viscosity, melting temperature, density, and heat capacities are of relevance. Because of the somewhat stronger tendency of D_2O to form hydrogen bonds, and thus a stronger structuring, the higher viscosity and density can be seen to be responsible for the measurable differences in the dynamic parameters of the spin probes in both solvents by spectroscopic methods.

The good agreement between simulation and the analysis of the parameters of the experimental ESR spectra shows that the effects of line broadening and line shift are mainly determined by spin exchange. In other words, the quantitative treatment of the spin exchange is useful to reflect sensitively the influence of the solvents on the dynamics of free radicals. In particular, this is true for discussing isotopic effects in solvents as it is shown in the present paper for the first time.

For example, this could be shown by means of influence of H_2O and D_2O on the habitus of the ESR spectra of the three differently polar spin probes TEMPO, TEMPOL, and CAT-1.

In particular, the low polarity of the spin probe TEMPO favors the process of differentiation between the two solvents. Even the variation of the microwave frequency (9.2 and 1.4 GHz) was advantageous, because it provided an additional parameter that changes the influence of the degree of anisotropy of the spin coupling parameters $\hat{g}$ and $\hat{A}$. Finally, this has been used for confirming the validity of the different models for the interpretation of the spectra.

The generally smaller values for k_e of the spin probe solutions in D_2O express the higher degree of structuring in that system, and thus the higher values for viscosity and density, too. Comparing the k_e values for the three spin probes, one can observe smaller values for the polar probes CAT-1 and TEMPOL, which can be explained with the better solvation than that of the nonpolar TEMPO. The latter will be less solvated and the probability to take part in forming hydrogen bonds will be smaller; thus it will be forced to stronger mutual interactions already at relatively low concentration, and resulting in larger k_e values.

AUTHOR INFORMATION

Corresponding Author

*Fax: +49 30 83850685. Phone: +49 30 83850695. E-mail: wfh@zedat.fu-berlin.de.

REFERENCES

(1) Pahlke, A. Physikalische und chemische Eigenschaften von leichtem und schwerem Wasser — untersucht am Beispiel des Spinaustausches von stabilen Radikalen. *B.Sc. Theses*, Humboldt University, Berlin, 2010.

(2) Ludwig, R.; Paschek, D. Anomalien und Rätsel - Wasser. *Chem. Unserer Zeit* **2005**, *39*, 164–175.

(3) Nemethy, G.; Scheraga, H. A. Structure of Water and Hydrophobic Bonding in Proteins. IV. The Thermodynamic Properties of Liquid Deuterium Oxide. *J. Chem. Phys.* **1964**, *41*, 680–689.

(4) Zhang, Y.; Faraone, A.; Kamitakahara, W. A.; Liu, K.-H.; Mou, C.-Y.; Leão, J. B.; Chang, S.; Chen, S.-H. Density hysteresis of heavy water confined in a nanoporous silica matrix. *Proc. Natl. Acad. Sci. U. S. A.* **2011**, *108*, 12206–12211.

(5) Seol, J.; Lee, J.-W.; Kim, D.-Y.; Takeya, S.; Ripmeester, J. A.; Lee, H. Molecular Cage Occupancy of Clathrate Hydrates at Infinite Dilution: Experimental Determination and Thermodynamic Significance. *J. Phys. Chem. B* **2010**, *114*, 804–808.

(6) Susilo, R.; Alavi, S.; Lang, S.; Ripmeester, J.; Englezos, P. Interactions between Structure H Hydrate Formers and Water Molecules. *J. Phys. Chem. C* **2008**, *112*, 9106–9113.

(7) Susilo, R.; Alavi, S.; Ripmeester, J.; Englezos, P. Tuning methane content in gas hydrates via thermodynamic modeling and molecular dynamics simulation. *Fluid Phase Equilib.* **2008**, *263*, 6–17.

(8) Perrin, C. L.; Flach, A. No Contribution of an Inductive Effect to Secondary Deuterium Isotope Effects on Acidity. *Angew. Chem.* **2011**, *123*, 7816–7818.

(9) Stösser, R.; Herrmann, W.; Marx, U.; Brückner, A. Spin Exchange in Solutions of TEMPOL in n-Octanol and 1-Methyl-3-octylimidazolium Hexafluorophosphate in the Temperature Range from 300 to 500 K. *J. Phys. Chem. A* **2011**, *155*, 2939–2952.

(10) Weil, J. A.; Bolton, J. R. Electron Paramagnetic Resonance. *Elementary Theory and Practical Applications*, 2nd ed.; John Wiley & Sons, Inc.: Hoboken, NJ, 2007.

(11) Banerjee, D.; Bhat, S. N.; Bhat, S. V.; Leporini, D. ESR evidence for 2 coexisting liquid phases in deeply supercooled bulk water. *Proc. Natl. Acad Sci. U. S. A.* **2009**, *106*, 11448–11453.

(12) Banerjee, D.; Bhat, S. V. Vitrification, relaxation and free volume in glycerol−water binary liquid mixture: Spin probe ESR studies. *J. Non-Cryst. Solids* **2009**, *355*, 2433–2438.

(13) Banerjee, D.; Bhat, S. V. Spin Probe ESR Signature of Freezing in Water: Is it Global or Local? eprint arXiv:0810.4682 2008.

(14) Angell, C. A.; Shuppert, J.; Tucker, J. C. Anomalous properties of supercooled water. Heat capacity, expansivity, and proton magnetic resonance chemical shift from 0 to −38°. *J. Phys. Chem.* **1973**, *77*, 3092–3099.

(15) Salikhov, K. M.; Molin, Yu. N.; Sagdeev, R. Z.; Buchachenko, A. L. In *Spin Polarization and Magnetic Effects in Radical Reactions*; Molin, Yu. N., Ed.; Akadémiai Kiadó: Budapest, 1984; pp 291−299.

(16) Molin, Yu. N.; Salikhov, K. M.; Zamaraev, K. I. *Spin Exchange*; Springer: Berlin, Heidelberg, 1980.

(17) Salikhov, K. Contributions of Exchange and Dipole−Dipole Interactions to the Shape of EPR Spectra of Free Radicals in Diluted Solutions. *Appl. Magn. Reson.* **2010**, *38*, 237–256.

(18) Bales, B. L.; Peric, M. EPR Line Shifts and Line Shape Changes Due to Spin Exchange of Nitroxide Free Radicals in Liquids. *J. Phys. Chem. B* **1997**, *101*, 8707–8716.

(19) Chemerisov, S. D.; Kokorin, A. I.; Grinberg, O. Ya.; Lebedev, Ya. S. The Study of the Electron Spin Exchange Efficiency in Liquid Solutions of Radicals at Various EPR Frequencies. *Appl. Magn. Reson.* **1995**, *9*, 37–45.

(20) Herrmann, W.; Stößer, R.; Moll, K.-P.; Borchert, H.-H. Rates of Rotational Diffusion and Heisenberg Spin Exchange as Obtained from CW ESR and ESR Tomographic Experiments on Model Systems and Human Skin. *Appl. Magn. Reson.* **2005**, *28*, 85–106.

(21) Herrmann, W.; Stößer, R.; Borchert, H.-H. ESR imaging investigations of two-phase systems. *Magn. Reson. Chem.* **2007**, *45*, 496–507.

(22) Grampp, G.; Rasmussen, K. Solvent dynamical effects on the electron self-exchange rate of the $TEMPO^{\bullet}/TEMPO^{+}$ couple (TEMPO = 2,2,6,6-tetramethyl-1-piperidinyloxy radical) Part I. ESR-linebroadening measurements at T = 298 K. *Phys. Chem. Chem. Phys.* **2002**, *4*, 5546–5549.

(23) Abe, T.; Tero-Kubota, S.; Ikegami, Y. Theory of solvent effects on the hyperfine splitting constants in ESR spectra of free radicals. *J. Phys. Chem.* **1982**, *86*, 1358–1365.

(24) Stoesser, R.; Herrmann, W.; Zehl, A.; Laschewsky, A.; Strehmel, V. Microviscosity and Micropolarity Effects of Imidazolium Based Ionic Liquids Investigated by Spin Probes Their Diffusion and Spin Exchange. *Z. Phys. Chem.* **2006**, *22*, 1309–1342.

(25) Budil, D. E.; Lee, S.; Saxena, S.; Freed, J. H. Nonlinear-Least-Squares Analysis of Slow-Motion EPR Spectra in One and Two Dimensions Using a Modified Levenberg-Marquardt Algorithm. *J. Magn. Reson.* **1996**, *A 120*, 155–189.

(26) Kurban, M. R.; Peric, M.; Bales, B. L. Nitroxide spin exchange due to re-encounter collisions in a series of n-alkanes. *J. Chem. Phys.* **2008**, *129*, 064501.

(27) Némethy, G.; Scheraga, H. A. Structure of Water and Hydrophobic Bonding in Proteins. II. Model for the Thermodynamic Properties of Aqueous Solutions of Hydrocarbons. *J. Chem. Phys.* **1964**, *36*, 3401–3417.

(28) Némethy, G.; Scheraga, H. A. Structure of Water and Hydrophobic Bonding in Proteins. I. A Model for the Thermodynamic Properties of Liquid Water. *J. Chem. Phys.* **1964**, *36*, 3382–3400.

(29) Moll, K.-P.; Herrmann, W.; Stößer, R.; Borchert, H.-H. Changes of the Properties in the Upper Layers of Human Skin on Treatment with Models of Different Pharmaceutical Formulations—An Ex vivo ESR Imaging Study. *ChemMedChem* **2008**, *3*, 653–659.

(30) Arunan, E.; Desiraju, G. R.; Klein, R. A.; Sadlej, J.; Scheiner, S.; Alkorta, I.; Clary, D. C.; Crabtree, R. H.; Dannenberg, J. J.; Hobza, P.; Kjaergaard, H. G.; Legon, A. C.; Mennucci, B.; Nesbitt, D. J. Definition of the Hydrogen Bond. IUPAC Final Report Nov. 2009.

(31) Kestin, J.; Sengers, J. V.; Kangar-Parsi, B.; Levelt Sengers, J. M. H. Thermophysical Properties of Fluid H_2O. *J. Phys. Ref. Data* **1984**, *13*, 175–183.

(32) Kestin, J.; Sengers, J. V.; Kangar-Parsi, B.; Levelt Sengers, J. M. H. Thermophysical Properties of Fluid D_2O. *J. Phys. Ref. Data* **1984**, *13*, 601–609.

(33) Elvingson, C. Relaxation Kinetlcs of Sodium Tetradecyl Sulfate Micelles in H_20 and D_2O. *J. Phys. Chem.* **1987**, *91*, 155–1460.

(34) Bhat, S. N.; Sharma, A.; Bhat, S. V. Vitrification and Glass Transition of Water: Insights from Spin Probe ESR. *Phys. Rev. Lett.* **2005**, *95*, 235702.